Neurobiology of Stress 36 (2025) 100723

Contents lists available at ScienceDirect

Neurobiology of Stress

journal homepage: www.elsevier.com/locate/ynstr

The insular cortex-nucleus tractus solitarius glutamatergic pathway involved in acute stress-induced gastric mucosal damage in rats

Zepeng Wang [a], Xinyu Li [a], Yuanyuan Li [a], Xuehan Sun [a], Yuxue Wang [a], Tong Lu [b], Dongqin Zhao [a], Xiaoli Ma [b,*], Haiji Sun [a,**]

[a] Key Laboratory of Animal Resistance Biology of Shandong Province, School of Life Science, Shandong Normal University, 88# Wenhua Road, Jinan, 250014, China
[b] Research Center of Basic Medicine, Central Hospital Affiliated to Shandong First Medical University, Jinan, 250013, China

ARTICLE INFO

Handling Editor: Dr. John Cryan

Keywords:
Insular cortex
Nucleus tractus solitarius
Glutamatergic neurons
Gastric mucosal damage
RWIS

ABSTRACT

Previous studies have shown that acute stress-induced gastric mucosal damage is linked to excessive activation of parasympathetic nervous system. The Insular Cortex (IC), the higher centers of the parasympathetic nervous system, serves as both the integration site of gastric sensory information and play a crucial role in the regulation of gastric function. However, whether the IC is involved in Restraint water-immersion stress (RWIS)-induced gastric mucosal damage has not been reported. In this study, we examined the expression of neuronal c-Fos, PSD95 and SYN-1 protein expression in IC during RWIS by immunofluorescence and western blot techniques, as well as assessed IC blood oxygenation level dependant (BOLD) through functional MRI. Chemical genetics techniques specifically modulate the activity of IC glutamatergic neurons and IC-nucleus tractus solitary (NTS) glutamatergic pathway to elucidate their contributions to RWIS-induced gastric mucosal damage. The results showed that the expression of c-Fos, PSD95, and SYN-1 protein in IC increased significantly after RWIS, along with a noticeable enhancement in fMRI signal intensity. Furthermore, inhibiting IC glutamatergic neurons and the IC-NTS glutamatergic neural pathway resulted in a significant reduction in gastric mucosal damage, an increase in the expression of Occludin, Claudin-1, and PCNA in the gastric wall, while the expression of nNOS decreased and CHAT increased. These findings suggest that during RWIS, IC glutaminergic neurons are activated, promoting stress-induced gastric mucosal damage through the IC-NTS-vagal nerve pathway.

1. Introduction

In clinical settings, conditions such as physical trauma, cold and heat stimulation, shock, sepsis, or head damage can lead to stress gastric mucosal lesion (SGML). SGML is characterized by inflammatory erosion, gastric bleeding, among other symptoms, and is challenging to treat. It is a prevalent visceral complication following stressful events (Dongqin et al., 2020). Restraint water-immersion stress (RWIS) is a complex stressor that significantly impacts the psychological and physiological well-being of rats, leading to rapid development of stress-induced gastric damage (Toshikatsu et al., 1990). This model is frequently used in research on the SGMI.

A recent study found that transsynaptic rabies virus injection into the anterior wall of the stomach in rats revealed anatomical connections between the cerebral cortex and the stomach (Clifford, 2002; Erik, 2011; Hugo and Neil, 2013; Marcelo et al., 2020). In the parasympathetic nervous system pathway that controls the stomach, first-level neurons are located in the dorsal nucleus of the vagus motor, second-level neurons in the nucleus of the solitary tract, and third-level neurons in the IC. It was found that the rostral segment of the IC is the main cortical source of parasympathetic nerve output to the stomach (Levinthal and Strick, 2020). The IC serves as the key "cortical motor center" of the parasympathetic nervous system that regulates gastric function. Through this descending pathway, the IC can regulate gastric motility, secretion, gastric mucosal permeability, and the release of signaling molecules in the gastric cavity, thus affecting gastric function. Our related studies have shown that c-Fos expression in multiple brain regions, including the dorsal complex of vagus nerve (DVC), nucleus tractus solitary, supraoptic nucleus, paraventricular nucleus, amygdala, paracarpal nucleus, periaqueductal gray matter and spinal cord significantly increased in the RWIS rats (Gao et al., 2021; Sun et al., 2018). The IC, one of the main high-level centers regulating visceral function, has anatomical

* Corresponding author. Central Hospital Affiliated to Shandong First Medical University, China.
** Corresponding author. Shandong Normal University, China.
E-mail addresses: Maxiaoli_jn@sdu.edu.cn (X. Ma), sunhj5018@126.com (H. Sun).

https://doi.org/10.1016/j.ynstr.2025.100723
Received 8 October 2024; Received in revised form 22 February 2025; Accepted 30 March 2025
Available online 1 April 2025

connections with the aforementioned brain regions. However, its involvement in stress-induced gastric mucosal damage has not been documented.

In this study, the expressions of c-Fos, PSD-95 and SYN-1 proteins in the IC were detected by immunofluorescence and western blot, and blood oxygenation level dependent (BOLD) in the IC was detected by fMRI to investigate whether the IC was involved in stress-induced gastric mucosal damage. Furthermore, adeno-associated virus vector was used to label IC glutamatergic neurons to explore their potential role in RWIS-induced gastric mucosal damage. In addition, we used chemical genetics to specifically inhibit or activate IC glutamatergic neurons, shedding light on their contribution to the damage caused by RWIS. Adeno-associated viral tools were then utilized to investigate the presence of glutamatergic projections from the IC to NTS, and to selectively modulate their activity. This approach aimed to elucidate the role of IC-NTS glutamatergic pathway in RWIS-induced gastric mucosal damage.

2. Materials and methods

2.1. Animal models

Wistar male rats, weighing 280–300 g, were provided by Jinan Pengyue Experimental Animal Breeding Co., LTD. The animals were randomly divided into three groups (each group/n = 6): control group and experimental group. The experimental groups were given RWIS 1h and 3h, respectively. After the rats were lightly anesthetized with ether, their limbs were bound with medical tape and fixed in the back position on a homemade board. Once the animals regained consciousness, they were placed in a 'standing position' in cold water at a controlled temperature of (21 ± 1) °C, with the water level reaching the xiphoid process of the sternum. All experimental procedures adhered to the ethical guidelines set by the International Association for the Study of Pain (Zimmermann, 1986) and approved by the Experimental Animal Ethical Association of Shandong Normal University (Number of the Animal Experimentation Ethics Committee: AEECSDNU, 2021023).

2.2. fMRI

The rat brain was initially positioned and adjusted on the scanning bed based on positioning images. T2-weighted scanning (T2WI) was then conducted with specific parameters: TR/TE: 4200/35ms, FOV: 30 × 30 mm, Averages: 1, Image size: 256 × 256, Slices: 38, Slice Thickness: 0.7 mm. Following the scanning, gas anesthesia was ceased, allowing the animal's heart rate to return to 80 beats/min. The T2WI sequence parameters were replicated for a band around 0.3 mm from the skull, ensuring even magnetic field distribution during scanning. BOLD-fMRI sequence scanning was performed with parameters such as Echo Time: 13000ms, Repetition Time: 2200ms, Repetitions: 240, FOV: 30 × 30 mm, Averages: 1, Image size: 90 × 90, Slices: 38, Slice Thickness: 0.7 mm. The MRI data was processed using Brucker Paravision 6.0.1d software, converted to DICOM format, and exported for further analysis.

2.3. Stereotaxic surgery and virus injection

Male Wister rats were fasted for 24 h before surgery and had access to water. The rats were anesthetized with isoflurane, and dental brackets were used to fix their teeth while bilateral ear rods were used to stabilize their skulls. The position of the earbar was adjusted to ensure consistent readings on both sides. The coordinates for the injection sites were determined based on the rat brain atlas: for the IC site, bregma: +1.2 mm, lateral to bregma: ±5.5 mm, subdural: 7.0 mm; for the NTS site, bregma: 1.34 mm, lateral to bregma: ±0.8 mm, subdural: 7.8 mm 13.4 mm. Slow virus injection (0.5 μl) began after a 6–8 min wait, with a constant flow rate of 0.05 μl/min. The needle was left in place for 10 min post-injection. Following bilateral injections, wounds were closed with sterilized sutures. Penicillin was administered daily for 3 days post-surgery to prevent infection.

2.4. Immunofluorescence

Coronal frozen sections of the brain, each 30 μm thick, were obtained in 0.01 mol/L PBS. To block endogenous enzyme activity, the sections were incubated in 0.01M PBS with 0.3 % Triton X-100 and 5 % normal goat serum (NGS) for 30 min at room temperature. Subsequently, the sections were incubated overnight at 4 °C with three primary antibodies, including rabbit anti-c-Fos (1:500; Abcam Biotechnology, UK). Following this, the sections underwent a 2-h incubation at room temperature with a biotin-labeled goat anti-rabbit IgG secondary antibody dilution. Negative control experiments utilized 0.01M PBS in place of the primary antibody.

2.5. Western blot

After RWIS, brain or stomach tissues were collected and protein was extracted. Protein extracts were separated by SDS-PAGE and then transferred to PVDF membranes. Subsequently, the membranes were blocked overnight at 4 °C with blocking solution (5 % skim milk powder and 0.1 % Tween-20 in 0.01 M PBS). After incubation at 4 °C overnight, rabbit anti-β-actin (1:8000; Huabio; Hangzhou, China), rabbit Occludin (1:1000; Huabio; Hangzhou, China), mouse anti- Claudin-1 (1:1000; Huabio; Hangzhou, China), rabbit anti-PCNA(1:5000; Proteintech,USA), rabbit anti-nNOS(1:500; Huabio; Hangzhou, China), rabbit anti-CHAT (1:500; Huabio; Hangzhou, China), rabbit anti-PSD95 (1:1000; Huabio; Hangzhou, China), rabbit anti-SYN-1 (1:1000; Huabio; Hangzhou, China). After rinsing three times in TBST buffer, the membranes were incubated with secondary antibodies for 1h at room temperature, the blots were detected by enhanced chemiluminescence, and the optical density (OD) values were measured by scanning with image analysis software.

2.6. Evaluation of gastric mucosal damage

Animals were sacrificed at the end of RWIS and the stomach was removed. Then, the stomach was gently cut along the greater curvature of the stomach, the gastric contents were washed out with normal saline, and the gastric wall was flattened. The mucus and blood clots on the gastric mucosa were wiped with a small cotton ball, and the degree of gastric mucosal damage was observed under an anatomical microscope. The erosion index (EI) was measured according to the methods of Guth (1992). Scores were obtained according to the length of the lesion: the length ≤1 mm as 1 score, 1 mm < the length ≤2 mm as 2 score, and the others were deduced in turn. The score was multiplied by 2 when the width of the lesion was larger than 1 mm. The cumulative score of EI for each rat is the gastric mucosal injury index of the animal.

2.7. Statistical analysis

SPSS25.0(SPSS Inc. Chicago, Ill, USA) statistical analysis software was used to process the data, and the experimental data of each group were expressed as mean ± standard error (x ± sem). The normality of measures was assessed using a Shapiro-Wilk test. We used an unpaired *t*-test for comparison between two groups, one-way analysis of variance (ANOVA) followed by LSD post hoc test for comparison among ≥3 groups, $P < 0.05$: a significant difference, $P < 0.01$: a very significant difference.

3. Results

3.1. The IC is involved in RWIS stress

To investigate the effects of RWIS on IC neurons, immunofluorescence and western blot techniques were used to detect the expression of

neuronal activation marker c-Fos and synaptic plasticity related proteins PSD-95 and SYN-1. fMRI was used to detect the BOLD of the IC. The blood oxygenation level dependent signal map is shown (Fig. 1A–C), revealing a significant enhancement in IC signal intensity in the stress 1-h group compared with the control group. Compared with the control group, the number of c-Fos-IR neurons in all segments of the IC significantly increased in both 1-h and 3-h stress groups. Interestingly, a decrease in the number c-Fos-IR neurons was observed in the rostral and middle segments of the IC in the 3-h stress group compared to the 1-h stress group, suggesting a time-dependent change in c-Fos-IR neuron expression ($F_{(2,15)} = 17.36$, **p < 0.01, ##p < 0.01, Fig. 1 D and G; $F_{(2, 15)} = 9.156$, **p < 0.01, #p < 0.05, Fig. 1 E and H; $F_{(2, 15)} = 6.575$, **p < 0.01, #p < 0.05, Fig. 1F and I). The expression of PSD-95 and SYN-1 protein was shown in Western blot (Fig. 1J), with a significant increase in PSD-95 protein expression in the IC of the 1-h stress group, while SYN-1 protein expression was elevated in both the 1-h and 3-h stress groups ($F_{(2, 15)} = 4.046$, *p < 0.05, Fig. 1K; $F_{(2, 15)} = 28.89$, **p < 0.01, ##p < 0.01, Fig. 1 L). Furthermore, the peak expression of PSD-95 and SYN-1 proteins was observed at 1 h of stress. These results indicate the involvement of the IC in the RWIS process.

3.2. IC glutaminergic neurons regulate RWIS-induced gastric mucosal damage

To investigate whether IC glutamatergic neurons are involved in RWIS, we utilized pAAV-CaMKIIa-mCherry to label glutamatergic neurons in IC. The activation of IC glutamatergic neurons was assessed by examining c-Fos co-localization with mCherry fluorescent signals (Fig. 2A). The results showed that, compared with the control group, the co-localization number and rate of CaMKIIa+ and c-Fos+ in the IC was significantly increased in the 1h and 3h stress groups ($F_{(2, 15)} = 25.18$, **p < 0.01, Fig. 2B; $F_{(2, 15)} = 39.33$, **p < 0.01, Fig. 2C), indicating the activation and involvement of IC glutamatergic neurons in RWIS.

To explore the role of IC glutamatergic neurons in RWIS-induced gastric mucosal damage, pAAV-CaMKIIa-hM4D (Gi)-mCherry was stereogenetically injected into the IC of rats to inhibit glutamatergic neurons. After RWIS 1h, the expression of c-Fos in the IC was detected by immunofluorescence (Fig. 3A–E). The results showed that the expression of c-Fos in the experimental group was significantly lower than that in control group ($F_{(2, 15)} = 14.76$, **p < 0.01, ##p < 0.01, Fig. 3F–I), indicating that the IC neurons were inhibited. The results showed that compared with the control group, the gastric erosion index in the experimental groups was significantly decreased ($F_{(2, 15)} = 17.90$, **p < 0.01, ##p < 0.01, Fig. 3J–M). Western blot analysis showed a significant increase in the expression of Occludin, Claudin-1 and PCNA in the stomach in comparison to the control groups ($F_{(2, 12)} = 13.16$, **p < 0.01, ##p < 0.01, Fig. 3O; $F_{(2, 12)} = 19.74$, **p < 0.01, ##p < 0.01, Fig. 3P; $F_{(2, 12)} = 42.65$, **p < 0.01, ##p < 0.01, Fig. 3Q). Additionally, the expression of nNOS and CHAT in the stomach was detected, showing a notable increase in CHAT expression in the experimental group compared to the control groups, while nNOS expression was significantly reduced ($F_{(2, 12)} = 89.79$, **p < 0.01, ##p < 0.01, Fig. 3R; $F_{(2, 12)} = 11.81$, **p < 0.01, ##p < 0.01, Fig. 3S). These findings suggest that inhibition of IC glutamate neurons could ameliorate gastric mucosal damage induced by RWIS through regulating the activity of intragastric neurons. Furthermore, the pAAV-CaMKIIa-hM3D (Gq)-mCherry was stereotactically injected into the IC of rats to activate glutamatergic neurons.

The experimental group was intraperitoneally injected with CNO, and the control group was injected with normal saline, followed by RWIS 1h. The injection site was identified as shown in (Fig. 4A–E). Immunofluorescence analysis revealed a significant increase in c-Fos expression in the IC of the experimental group compared to the control groups, saline ($F_{(2, 15)} = 12.09$, *p < 0.05, ##p < 0.01, Fig. 4F–I), indicating that the IC neurons were activated. Furthermore, there was no significant difference in gastric erosion index between the experimental and the control groups (Fig. 4J–M). Western blot analysis revealed a significant decrease in the expression of Occludin, Claudin-1 and PCNA in the experimental groups compared to the control group ($F_{(2, 15)} = 10.29$, **p < 0.01, ##p < 0.01, Fig. 4O; $F_{(2, 15)} = 8.121$, **p < 0.01, ##p < 0.01, Fig. 4P; $F_{(2, 15)} = 14.16$, **p < 0.01, #p < 0.05, Fig. 4Q). Additionally, the expression of nNOS and CHAT in the stomach was detected. The results showed that compared with the control groups, the expression of CHAT in the experimental groups was significantly decreased, while nNOS expression was significantly increased ($F_{(2, 15)} = 46.39$, **p < 0.01, ##p < 0.01, Fig. 4R; $F_{(2, 15)} = 12.10$, **p < 0.01, ##p < 0.01, Fig. 4S), indicating that activation of IC glutamate neurons disrupted gastric mucosal tight junction structures but did not alter gastric mucosal damage. These results suggest that during RWIS, IC glutaminergic neurons are activated, *aggravating* stress-induced gastric mucosal damage.

3.3. IC glutamatergic neurons project to the NTS

To investigate a potential glutamatergic projection connection between the IC and the NTS, the rat IC was injected with pAAV-CaMKIIa-mCherry to label glutamatergic neurons in the IC. The results showed that there were obvious red fluorescent nerve fibers in the bilateral NTS, indicating the presence of glutamatergic neural projections from the IC to the NTS (Fig. 5A–G).

To investigate whether IC glutamatergic neurons have a role in regulating the NTS in RWIS, Stereotaxic injection of pAAV-CaMKIIa-hM4D (Gi)-mCherry/pAAV-CaMKIIa-hM3D (Gq)-mCherry, specifically inhibited or activated glutamatergic neurons. Immunofluorescence detection of c-Fos expression in the NTS showed that Compared with control group, the expression of c-Fos in the nucleus of the solitary tract and the dorsal nucleus of the vagus nerve was significantly decreased after inhibition of the IC glutamatergic neurons ($F_{(2, 15)} = 11.30$, *p < 0.05, ##p < 0.01, Fig. 5K; $F_{(2, 15)} = 11.25$, **p < 0.01, ##p < 0.01, Fig. 5L). Conversely, and the expression of c-Fos in the nucleus of the solitary tract and the dorsal nucleus of the vagus nerve was significantly increased after activation of the IC glutamatergic neurons ($F_{(2, 15)} = 34.62$, **p < 0.01, ##p < 0.01, Fig. 5P; $F_{(2, 15)} = 15.45$, **p < 0.01, ##p < 0.01, Fig. 5Q). These results suggest that activation or inhibition of the activity of glutamatergic neurons in the IC can alter the activity of the NTS accordingly.

3.4. The glutaminergic pathway of the IC-NTS regulates RWIS-induced gastric mucosal damage

To further investigate whether IC glutamatergic neurons regulate RWIS-induced gastric mucosal damage through the NTS, rats were stereotactically injected with AAV2-retro-CaMKIIa-Cre into the NTS in rats and AAV9-CaMKIIa-DIO-hM4D (Gi)-mCherry into the IC. This injection aimed to inhibit the glutaminergic pathway of the IC-NTS. The injection site was identified as shown in (Fig. 6A–C). Immunofluorescence was used to detect the expression of RWIS-induced c-Fos in the IC and NTS. The results showed that the expression of c-Fos in the experimental group was significantly lower than that in the control group ($F_{(2, 15)} = 17.99$, **p < 0.01, ##p < 0.01, Fig. 6G; $F_{(2, 15)} = 33.48$, **p < 0.01, ##p < 0.01, Fig. 6K), indicating that the neurons of the IC and NTS were inhibited. Furthermore, compared with the control groups, the gastric erosion index of the experimental group was significantly decreased ($F_{(2, 15)} = 33.94$, **p < 0.01, ##p < 0.01, Fig. 6L–O). Western blot analysis demonstrated a significant increase in the expression of Occludin, Claudin-1, and PCNA in the experimental group relative to the control group ($F_{(2, 15)} = 23.92$, **p < 0.01, ##p < 0.01, Fig. 6Q; $F_{(2, 15)} = 10.05$, **p < 0.01, ##p < 0.01, Fig. 6R; $F_{(2, 15)} = 33.43$, **p < 0.01, ##p < 0.01, Fig. 6S). Additionally, the expression of nNOS and CHAT in the stomach was detected. The expression of intragastric CHAT in the experimental groups was significantly increased in compared to the control group. Conversely, the expression of nNOS was significantly

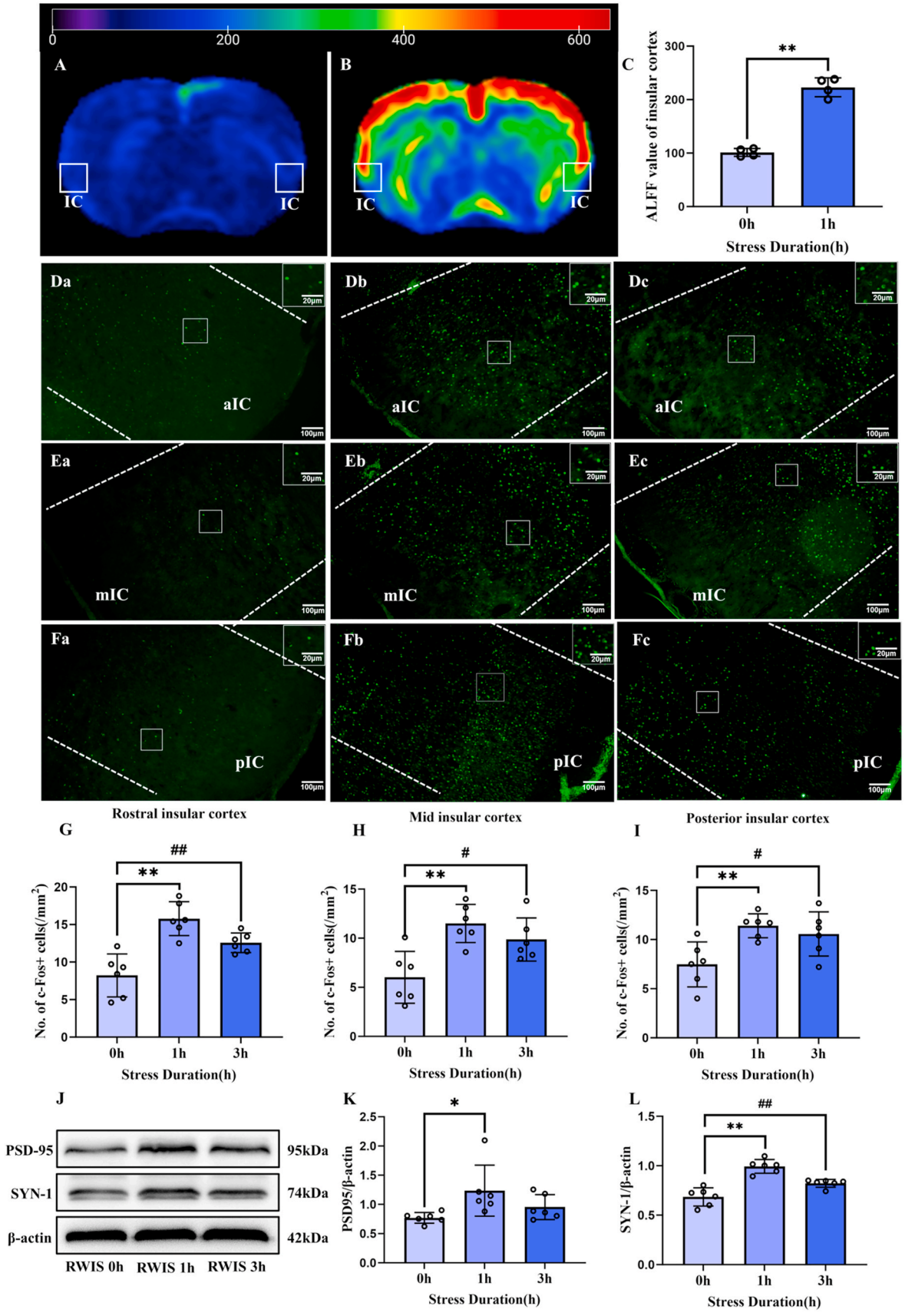

(caption on next page)

Fig. 1. The IC is involved in RWIS stress. A: ALFF signal in the IC induced by RWIS 0h; B: ALFF signal in the IC induced by RWIS 1h; C: Quantification of the ALFF value, compared with control group, **: P < 0.01; (n = 4) Da-Dc: c-Fos-IR neurons in the rostral IC induced by RWIS at 0 h, 1 h and 3 h (a: control group; b: stress 1h group; c: stress 3h group); Ea-Ec: c-Fos-IR neurons in the middle IC induced by RWIS at 0 h, 1 h and 3 h; Fa-Fc: c-Fos-IR neurons in the caudal IC induced by RWIS at 0 h, 1 h and 3 h (100 x); scale bar, 100 μm c-Fos in a rectangle were magnified to a higher magnification (400 ×); scale bar, 20 μm; G–I: The number of c-Fos-IR neurons in the rostral, middle and caudal IC was quantified, the stress of 1 h group compared with control group, stress *: P < 0.05, **: P < 0.01, the stress of 3 h group compared with control group, #: P < 0.05, ##: P < 0.01 (n = 6) J: Western blot of PSD-95 and SYN-1 protein induced by RWIS; K–L: Quantification of the relative average grayscale value of PSD-95/β-actin and SYN-1/β-actin, the stress of 1 h group compared with control group, stress *: P < 0.05, **: P < 0.01, the stress of 3 h group compared with control group, #: P < 0.05, ##: P < 0.01 (n = 6).

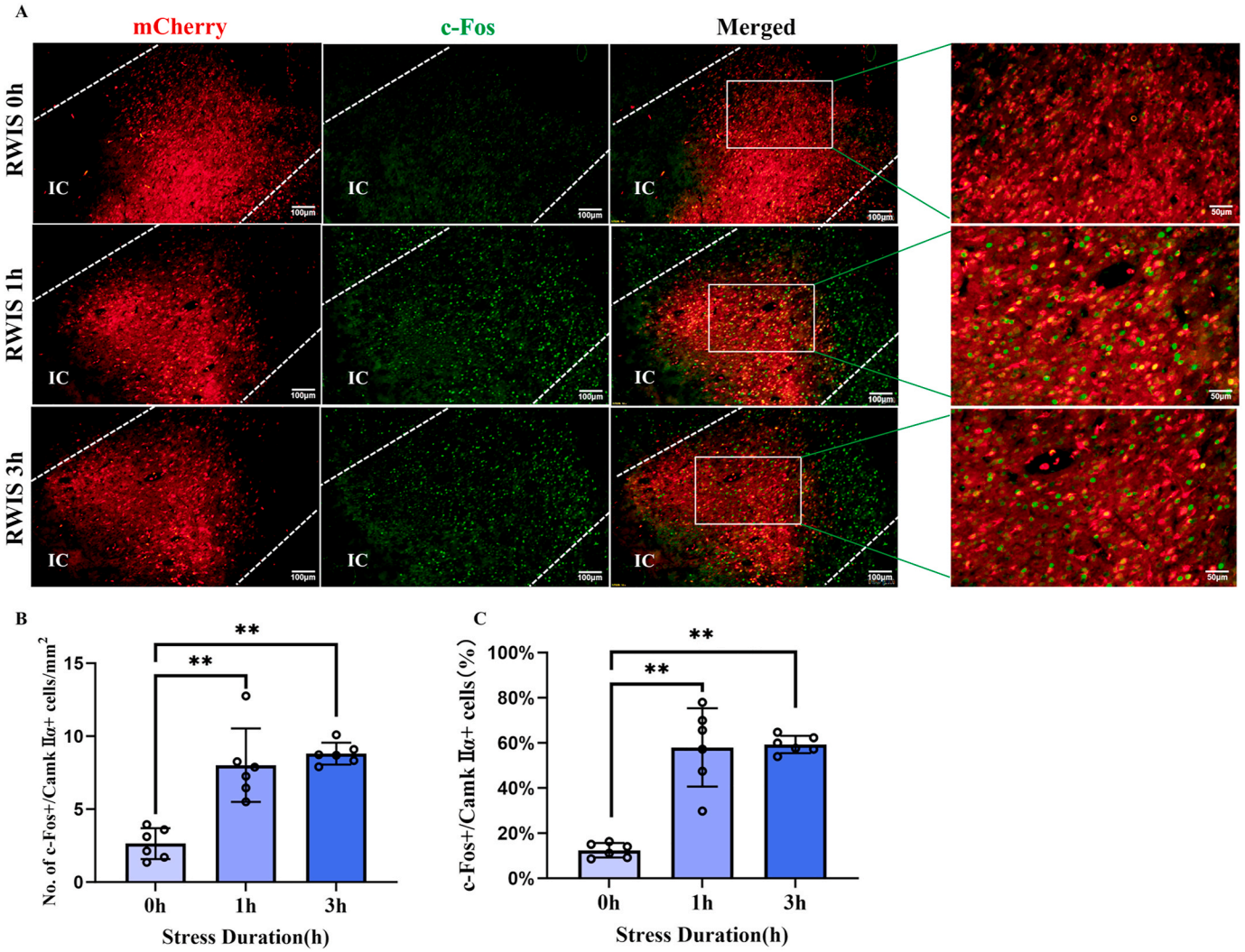

Fig. 2. IC glutaminergic neurons involved RWIS. A: CaMKIIa+/c-Fos + co-localization in the IC induced by RWIS at 0 h,1 h and 3 h of RWIS(100 x); scale bar, 100 μm CaMKIIa+/c-Fos + co-localization in a rectangle were magnified to a higher magnification (200 ×); scale bar, 50 μm; B: The number of CaMKIIa+/c-Fos + co-localization in the IC was quantified.compared with control group, each group **: P < 0.01 (n = 6); C: The rate of CaMKIIa+/c-Fos + co-localization in the IC was quantified. compared with control group, each group **: P < 0.01 (n = 6).

decreased ($F_{(2, 15)} = 9.722$, **p < 0.01, ##p < 0.01, Fig. 6T; $F_{(2, 15)} = 24.38$, **p < 0.01, ##p < 0.01, Fig. 6U). These findings indicate that inhibition of the IC-NTS glutamatergic pathway significantly ameliorated the gastric damage induced by RWIS and may change the activity of intragastric neurons.

Moreover, the rats received stereotaxic injection of AAV2-retro-CaMKIIa-Cre into the NTS and AAV9-CaMKIIa-DIO-hM3D (Gq)-mCherry into the IC to activate the glutamate neural pathway of the IC-NTS. After RWIS 1h, the injection site was identified (Fig. 7A–C), and the expression of c-Fos in the IC and NTS was detected by immunofluorescence. The results showed a significant increase in the expression of c-Fos in the experimental groups compared to the control group, indicating that the neurons in the IC and NTS were activated ($F_{(2, 15)} = 19.70$, **p < 0.01, ##p < 0.01, Fig. 7G; $F_{(2, 15)} = 13.64$, **p < 0.01, ##p < 0.01, Fig. 7K). Gastric erosion index did not differ significantly between the experimental group and the control group. (Fig. 7L–O). Western blot analysis of Occludin, Claudin-1 and PCNA expression in the stomach revealed no significant changes in experimental group compared to the control group (Fig. 7Q–S). Furthermore, the expression of nNOS and CHAT in the stomach was detected, showed no significant difference (Fig. 7T and U).

4. Discussion

In the present study, it was observed that RWIS activated glutamatergic neurons in the IC and caused changes in synaptic plasticity. In

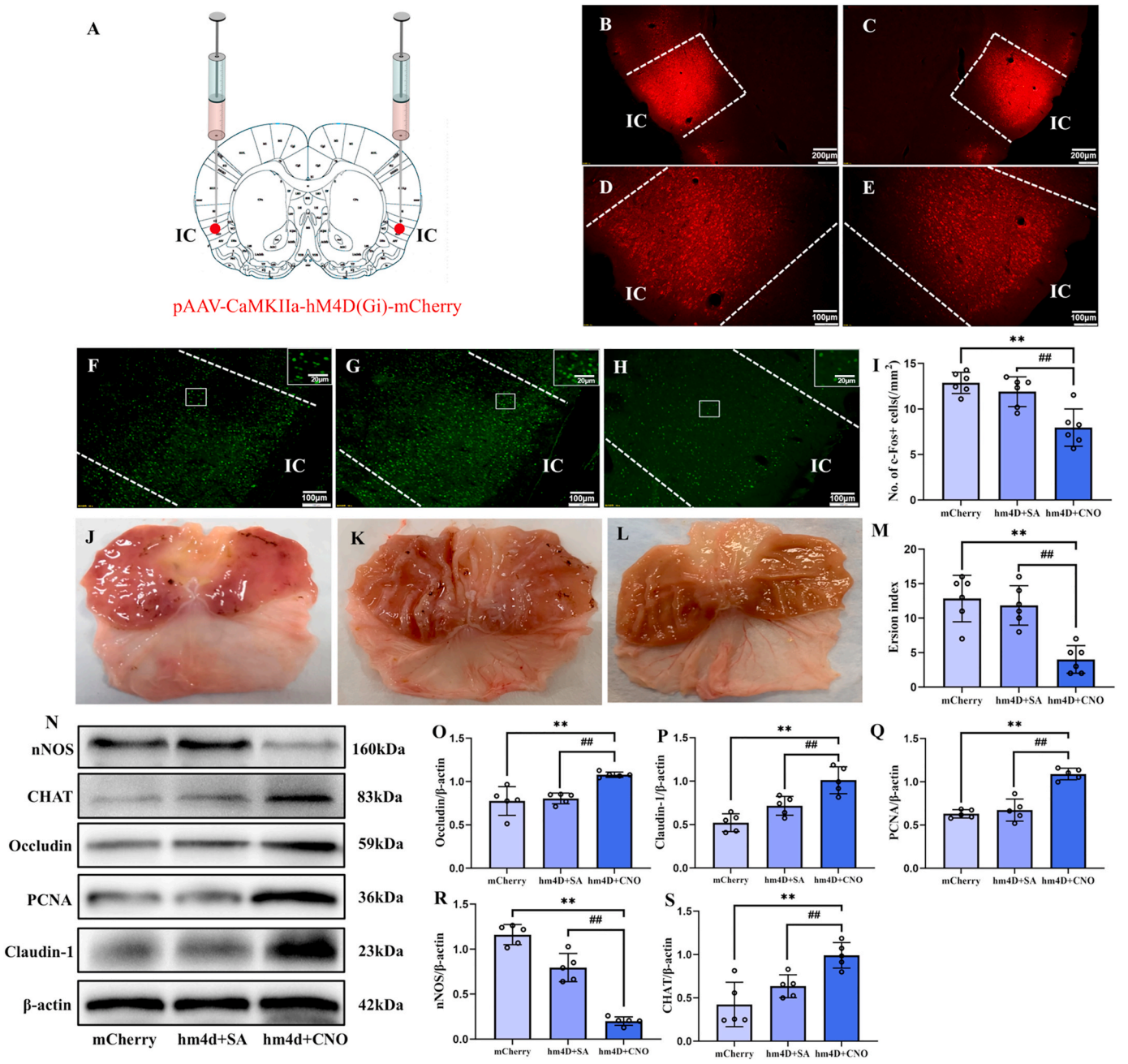

Fig. 3. Inhibition IC glutamate neurons to the influence of the gastric mucosa damage induced by RWIS. A: Schematic of virus injection; B–C: Viral expression in the left and right IC (40 ×) scale bar, 200 μm; D–E: Viral expression in the left and right IC (100 ×) scale bar, 100 μm; F: c-Fos expression in RWIS rats treated with CaMKIIa-mCherry in the IC; G–H: c-Fos expression in RWIS rats in the IC of the CaMKIIa-hm4d + saline- or CNO-injected groups (100 ×). scale bar,100 μm, c-Fos in a rectangle were magnified to a higher magnification (400 ×); scale bar, 20 μm; I: The number of c-Fos-IR neurons in the IC was quantified. compared with mCherry group, *: $P < 0.05$, **: $P < 0.01$, compared with hm4d + SA group, #: $P < 0.05$, ##: $P < 0.01$ (n = 6); J: Gastric mucosal damage in RWIS rats treated with CaMKIIa-mCherry; K–L: Gastric mucosal damage in RWIS rats in the IC of the CaMKIIa-hm4d + saline- or CNO-injected groups; M: Quantification of erosion index (EI). compared with mCherry group, *: $P < 0.05$, **: $P < 0.0$, compared with hm4d + SA group, #: $P < 0.05$, ##: $P < 0.01$ (n = 6); N: Western blot of Occludin, Claudin-1, PCNA, NOS and CHAT protein expression in different groups; O–S: Quantification of the relative average grayscale value of Occludin/β-actin, Claudin-1/β-actin, PCNA/β-actin, NOS/β-actin and CHAT/β-actin. compared with the mCherry group, *: $P < 0.05$, **: $P < 0.01$, compared with hm4d + SA group, #: $P < 0.05$, ##: $P < 0.01$ (n = 5).

addition, specific inhibition of IC glutamatergic neurons significantly reduced RWIS-induced gastric mucosal damage, indicating that activation of IC glutamatergic neurons causes RWIS-induced gastric mucosal damage. Furthermore, we found that there was an IC-NTS glutamatergic projection, and that the activation of IC-NTS glutamatergic pathway causes RWIS-induced gastric mucosal damage.

The IC, As a crucial part of the cerebral cortex, plays a key role in processing various sensory information, such as viscera, taste, somatic response, and hearing (Yu et al., 2020). As the primary source of parasympathetic output, the IC forms direct connections with the stomach through the NTS. Our previous study demonstrated that the NTS are involved in RWIS-induced gastric mucosal damage. Due to the close relationship between the NTS and the IC in structure and function (Yuyu, 2009). It is possible that the IC participates in RWIS and contributes to stress-induced gastric mucosal damage. In this study, fMRI BOLD signal intensity in the IC was significantly increased after stress.

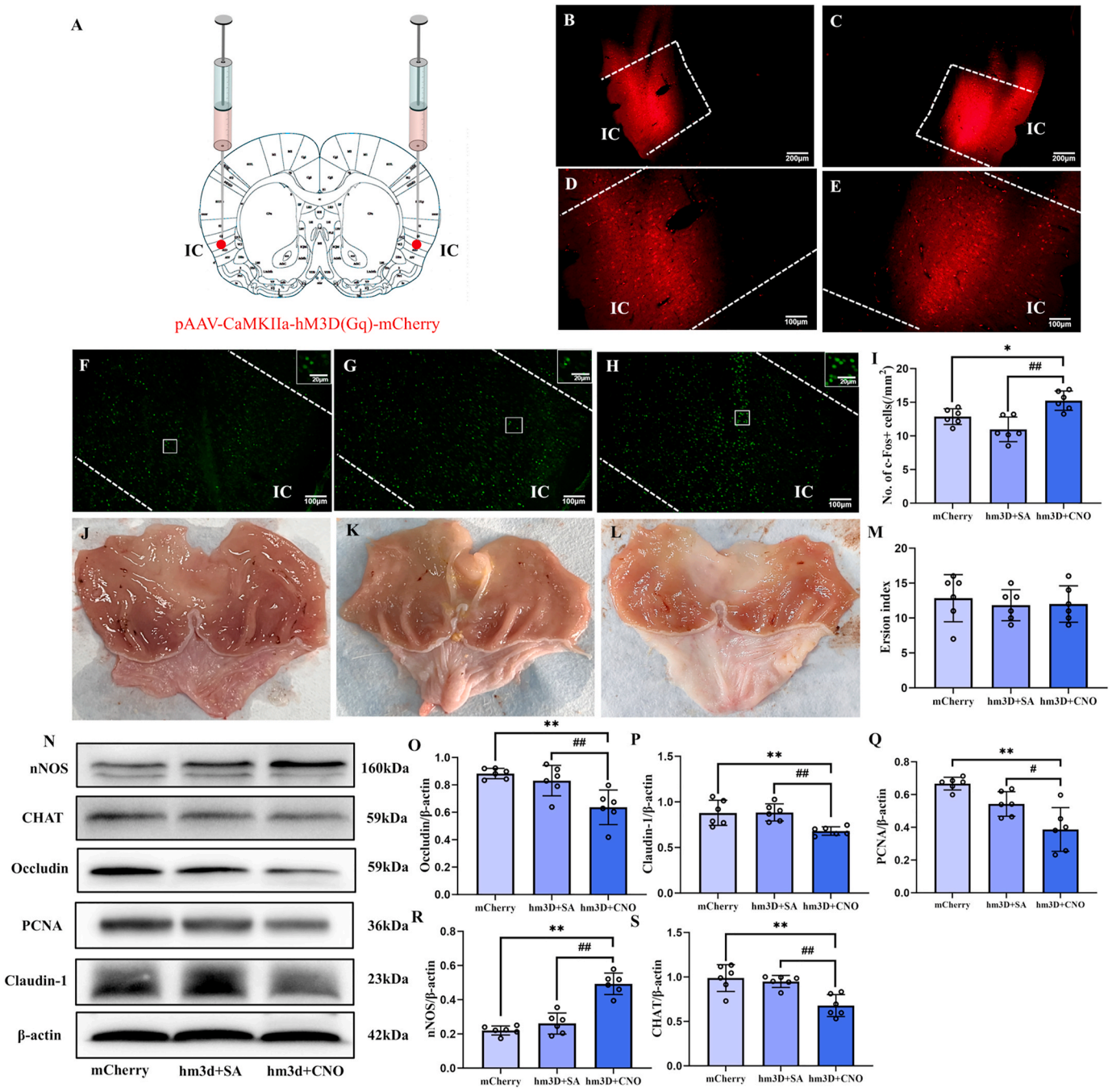

Fig. 4. Activation IC glutamate neurons to the influence of the gastric mucosa damage induced by RWIS. A: Schematic of virus injection; B–C Viral expression in the left and right IC (40 ×) scale bar, 200 μm; D–E: Viral expression in the left and right IC (100 ×) scale bar,100 μm; F: c-Fos expression in RWIS rats treated with CaMKIIa-mCherry in the IC; G–H: c-Fos expression in RWIS rats in the IC of the CaMKIIa-hm3d + saline- or CNO-injected groups (100 ×) scale bar,100 μm, c-Fos in a rectangle were magnified to a higher magnification (400 ×); scale bar, 20 μm; I: The number of c-Fos-IR neurons in the IC was quantified. compared with mCherry group, *: $P < 0.05$, **: $P < 0.01$, compared with hm3d + SA group, #: $P < 0.05$, ##: $P < 0.01$ (n = 6); J: Gastric mucosal damage in RWIS rats treated with CaMKIIa-mCherry; K–L: Gastric mucosal damage in RWIS rats in the IC of the CaMKIIa-hm3d + saline- or CNO-injected groups; M: Quantification of erosion index (EI). compared with mCherry group, *: $P < 0.05$, **: $P < 0.0$, compared with hm3d + SA group, #: $P < 0.05$, ##: $P < 0.01$ (n = 6); N: Western blot of Occludin, Claudin-1, PCNA, NOS and CHAT protein expression in different groups; O–S: Quantification of the relative average grayscale value of Occludin/β-actin, Claudin-1/β-actin, PCNA/β-actin, NOS/β-actin and CHAT/β-actin. compared with the mCherry group, *: $P < 0.05$, **: $P < 0.01$, compared with hm3d + SA group, #: $P < 0.05$, ##: $P < 0.01$ (n = 6).

Furthermore, we examined the expression of c-Fos in indifferent segments of the IC at various stress periods, revealing a significant increase in c-Fos expression after stress. Additionally, the levels of PSD95 and SYN-1 in the IC also showed varying increments following stress. These results indicate that the neurons in the IC are activatedduring RWIS and are involved in stress-induced gastric mucosal damage.

Glutamate is the main excitatory neurotransmitter in the central nervous system (Richard et al., 1999). Recent studies have shown that IC glutamatergic neurotransmission via NMDA receptors plays an important role in autonomic nervous system and cardiovascular responses induced by restraint stress (Melissa et al., 2022). Ming-Ming Zhang found that glutamatergic projections from the IC to the basolateral

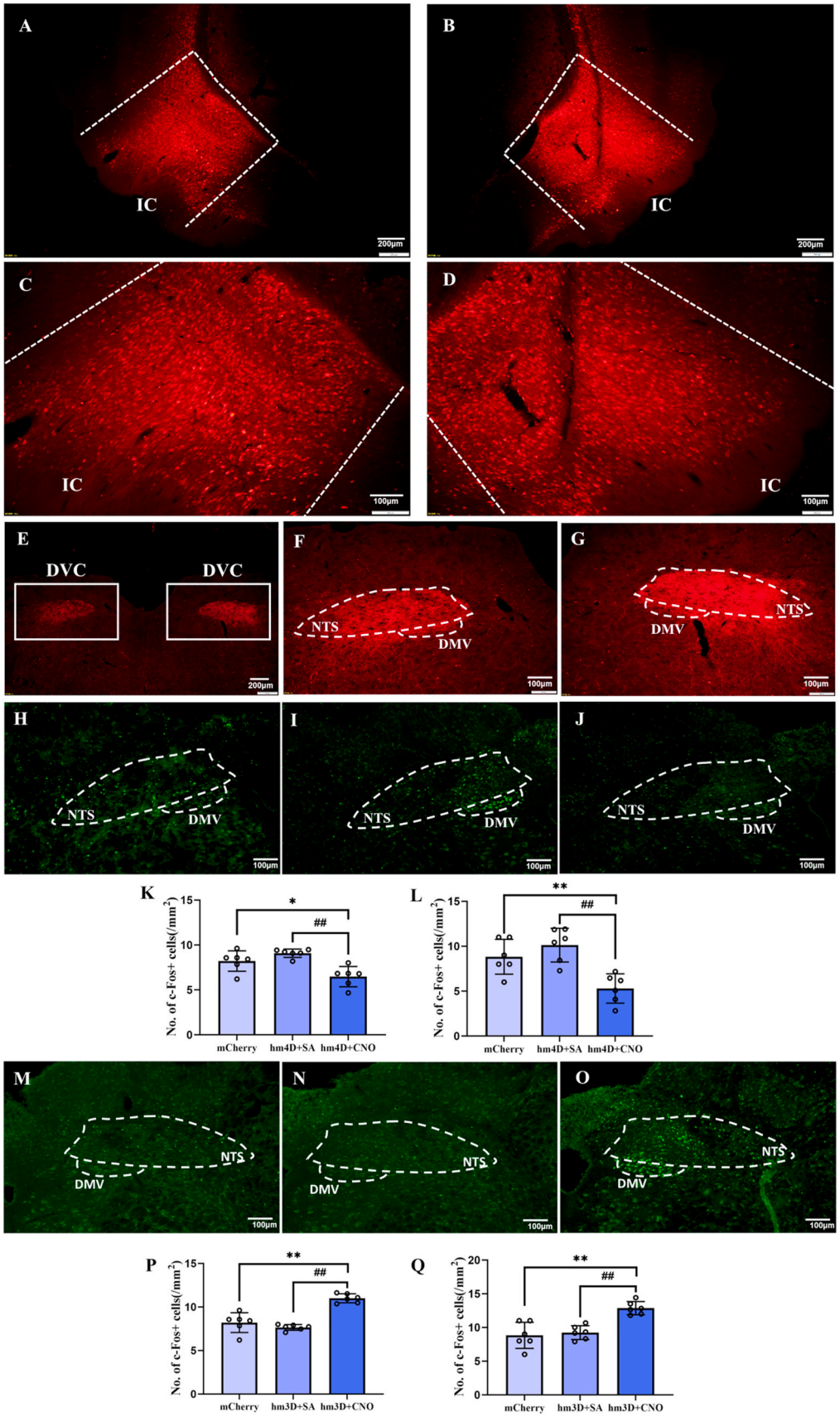

(caption on next page)

Fig. 5. The IC is associated with the DVC. A–B: viral expression in the left and right IC (40 ×) scale bar, 200 μm; C–D: viral expression in the left and right IC (100 ×) scale bar,100 μm; E: CamkIIa+ fibres in the bilateral DVC, (40 ×) scale bar, 200 μm; F–G: CamkIIa+ fibres in the bilateral DVC. (200 ×) scale bar,50 μm; H: c-Fos expression in RWIS rats treated with CaMKIIa-mCherry in the DVC; I–J: c-Fos expression in RWIS rats in the DVC of the CaMKIIa-hm4d + saline- or CNO-injected groups (100 ×). scale bar,100 μm; K: The number of c-Fos-IR neurons in the NTS was quantified; L: The number of c-Fos-IR neurons in the DMV was quantified. compared with mCherry group, *: $P < 0.05$, **: $P < 0.01$, compared with hm4d + SA group, #: $P < 0.05$, ##: $P < 0.01$ (n = 6); M: c-Fos expression in RWIS rats treated with CaMKIIa-mCherry in the DVC; N–O: c-Fos expression in RWIS rats in the DVC of the CaMKIIa-hm3d + saline- or CNO-injected groups (100 ×). scale bar,100 μm; P: The number of c-Fos-IR neurons in the NTS was quantified; Q: The number of c-Fos-IR neurons in the DMV was quantified. compared with mCherry group, *: $P < 0.05$, **: $P < 0.01$, compared with hm3d + SA group, #: $P < 0.05$, ##: $P < 0.01$ (n = 6).

amygdala (BLA) are involved in regulating observational pain formation in mice, and that selective activation or inhibition of the IC-BLA projection pathway enhances or attenuates the intensity of observational pain, respectively (Mingming et al., 2022; Zhang et al., 2023). In the present study, we examined changes of c-Fos+/CaMKIIa + colocalization in the IC during various stress periods. Our results showed a significant increase in the c-Fos+/CaMKIIa + colocalization in the IC following stress, indicating that the activity of IC glutamatergic neurons during RWIS might contribute to RWIS-induced gastric mucosal damage.

To further investigate the role of IC glutamatergic neurons in RWIS-induced gastric mucosal damage. We examined the expression of Occludin, Claudin-1, PCNA, nNOS and CHAT in the gastric wall after specific inhibition or activation of IC glutamatergic neurons by chemogenetic methods. Tight junctions (TJ) are crucial structural components of epithelial tissue, forming a physical barrier protects against external harmful substances and pathogens in the gastrointestinal tract. Tight junction proteins, including Claudins, Occludin, and zonula occludens (ZOs)(Udo and Schuetz, 2019), are essential for tight junction function, influencing barrier integrit, cell migration, invasion, anti-apoptosis and cell proliferation (Emanuela et al., 2002; Oluwole, 2015; Stelios et al., 2011). Our results showed that specific inhibition of IC glutamatergic neurons significantly ameliorated RWIS-induced gastric damage, increased gastric Occludin and Claudin expression in RWIS rsts. Activation of glutamatergic neurons in the IC did not cause significant changes in gastric damage, but the expression of Occludin and Claudin significantly decreased, indicating that activation of glutamatergic neurons in the IC would destroy the integrity of gastric mucosal barrier.

Proliferating cell nuclear antigen (PCNA) is closely related to cell proliferations (Elizabeth et al., 2016; Rodrigo and Julio, 1980). PCNA is essential in eukaryotic DNA replication, with activities observed in reactions such as DNA methylation and Okazaki fragment ligation (Rodrigo et al., 1981). A study on water-immersion and restraint stress-induced gastric mucosal damage in rats showed that the expression of PCNA decreased following stress, and after a period of recovery, the expression of PCNA gradually recovered (Jing et al., 2003), indicating that a correlation between decreased PCNA expression and gastric mucosal damage. Consistent with these findings, the expression of PCNA in RWIS rats was significantly increased after the inhibition of IC glutamatergic neurons, indicating that their repair function was activated to alleviate RWIS-induced gastric mucosal damage. Conversely, the expression of PCNA significantly decreased after the activation of IC glutamatergic neurons, and epithelial tissue repair ability was reduced, thus delaying the recovery of gastric mucosal injury.

There are various types of neurons in the Enteric Nervous System (ENS) that release different neurotransmitters. Gastrointestinal excitatory motor neurons release excitatory transmitters like ACh and SP, which promote gastrointestinal smooth muscle contraction and glandular secretion. In contrast, inhibitory motor neurons release inhibitory transmitters such as VIP and NO, which suppress gastrointestinal smooth muscle contraction and glandular secretion. These excitatory and inhibitory motor neurons in the gastrointestinal system can interact with each other in a complex and delicate balance. Disruption of this balance can lead to gastrointestinal dysfunction (Jia et al., 2017; Qiang et al., 2017; Zhou, 2004). NO is mainly produced from L-arginine catalyzed by nitric oxide synthase (NOS), which acts as the key rate-limiting enzyme for NO synthesis (Yuwei et al., 2017). Studies have found that NOS is widely distributed in the gastrointestinal tract. playing a role in regulating gastrointestinal function (Hongyu, 2005; Shun-Wu, 2009; Ying et al., 2014). In the present study, inhibition of IC glutamatergic neurons led to a significant decrease in gastric nNOS expression, an increase in CHAT expression, and a reduction in gastric mucosal damage. Conversely, activation of IC glutamatergic neurons results in decreased gastric CHAT expression, increased nNOS expression, but did not have an impact on gastric mucosal damage. These findings suggest that inhibiting IC glutamatergic neurons could potentially activate cholinergic neurons and suppress the activity of NO neurons in the gastric myenteric plexus, ultimately improving RWIS-induced gastric mucosal damage.

DVC including the dorsal vagus nucleus (DMV), nucleus tractus solitarius (NTS), and area postrema (AP) integrates visceral sensation and motor information, and participates in the regulation of gastric function. DVC play an important role in the occurrence of gastric mucosal damage. Zhang et al. found that the expression of c-Fos was increased in DVC at different time periods of RWIS (30,60,120 and 180min), with the highest intensity in the DMV, followed by NTS, which further confirmed that RWIS-induced gastric mucosal damage primarily stems from excessive activation of parasympathetic nerve system (Yuyu, 2009; Yvette et al., 1989). The IC, as an important part of autonomic nervous system, involved in the high-level processing of visceral sensory information and initiating autonomic responses (Yanwei et al., 2022). The retrograde tracer CTB was injected into the rat NTS, and CTB-labeled pyramidal neurons were detected in the IC cortex (Silvia et al., 2020), indicating a projective connection between the IC and the DVC that may influence stomach function. In the present study, injection of adeno-associated virus (AAV) into IC glutamatergic neurons resulted in the observation of fluorescently labeled nerve fibers in the NTS, and specific inhibition or activation of IC glutamatergic neurons resulted in corresponding changes of neuronal activity in the NTS and DMV. This study further confirms that the existence of glutamatergic projection connection between the IC and the NTS, and that the activity of IC glutamatergic neurons directly affects the NTS activity. Moreover, inhibition of the IC-NTS glutamatergic nerve pathway attenuated gastric bleeding, increased the expression of Occludin, Claudin-1 and PCNA, decreased the expression of nNOS, and increased the expression of CHAT, which was consistent with the results of inhibition of IC glutamatergic neurons alone, and significantly ameliorated gastric mucosal damage induced by RWIS. However, specific activation of the glutamatergic pathway of the IC-NTS did not change gastric bleeding, nor did the expression of Occludin, Claudin-1, PCNA, nNOS and CHAT, which did not significantly change RWIS-induced gastric mucosal damage.

In conclusion, the present study has demonstrated that IC glutaminergic neurons are activated, aggravating stress-induced gastric mucosal damage through the IC-NTS-vagal nerve pathway during RWIS (Fig. 8A–D). Our study provides a new direction for the central mechanism of SGML, while the specific molecular mechanisms of the involvement of IC glutamatergic neurons in RWIS-induced gastric mucosal damage require further investigation.

CRediT authorship contribution statement

Zepeng Wang: Writing – original draft, Validation, Project

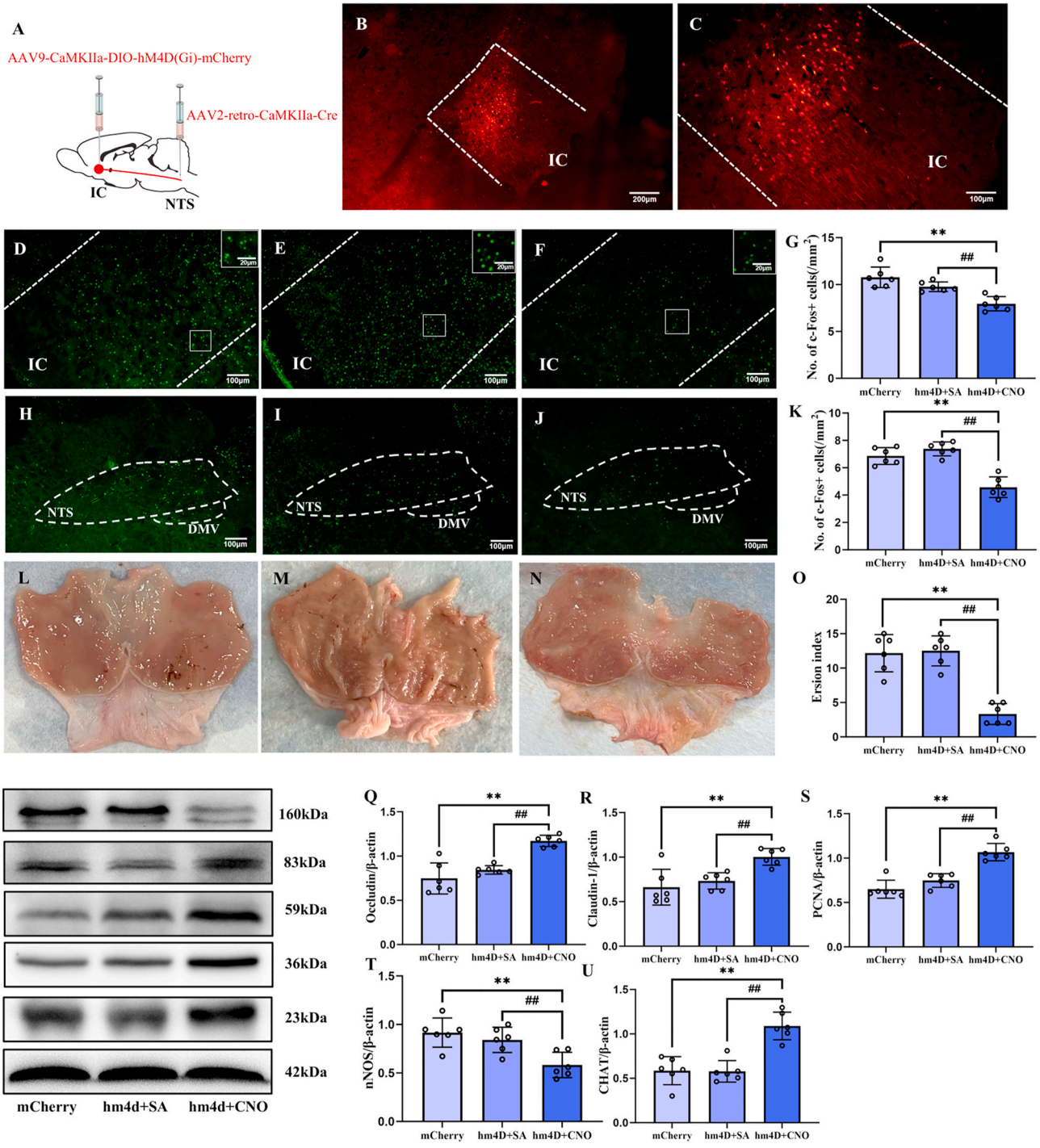

Fig. 6. Effect of inhibition of the IC-NTS glutamatergic pathway on RWIS-induced gastric mucosal damage.
A: Schematic of virus injection; B: Viral expression in the IC (40 ×) scale bar, 200 μm; C: Viral expression in the IC (100 ×) scale bar,100 μm; D: c-Fos expression in RWIS rats treated with CaMKIIa-mCherry in the IC; E–F: c-Fos expression in RWIS rats in the IC of the CaMKIIa-hm4d + saline- or CNO-injected groups (100 ×). scale bar,100 μm, c-Fos in a rectangle were magnified to a higher magnification (400 ×); scale bar, 20 μm; G: The number of c-Fos-IR neurons in the insul was quantified. compared with mCherry group, *: $P < 0.05$, **: $P < 0.01$, compared with hm4d + SA group, #: $P < 0.05$, ##: $P < 0.01$ (n = 6); H: c-Fos expression in RWIS rats treated with CaMKIIa-mCherry in the NTS; I–J: c-Fos expression in RWIS rats in the NTS of the CaMKIIa-hm4d + saline- or CNO-injected groups (100 ×). scale bar,100 μm; K: The number of c-Fos-IR neurons in the NTS was quantified. compared with mCherry group, *: $P < 0.05$, **: $P < 0.01$, compared with hm4d + SA group, #: $P < 0.05$, ##: $P < 0.01$ (n = 6); L: Gastric mucosal damage in RWIS rats treated with CaMKIIa-mCherry; M–N: Gastric mucosal damage in RWIS rats in the IC of the CaMKIIa-hm4d + saline- or CNO-injected groups; O: Quantification of erosion index (EI). compared with mCherry group, *: $P < 0.05$, **: $P < 0.0$, compared with hm4d + SA group, #: $P < 0.05$, ##: $P < 0.01$ (n = 6); P: Western blot of Occludin, Claudin-1, PCNA, NOS and CHAT protein expression in different groups; Q–U: Quantification of the relative average grayscale value of Occludin/β-actin, Claudin-1/β-actin, PCNA/β-actin, NOS/β-actin and CHAT/β-actin. compared with the mCherry group, *: $P < 0.05$, **: $P < 0.01$, compared with hm4d + SA group, #: $P < 0.05$, ##: $P < 0.01$ (n = 6).

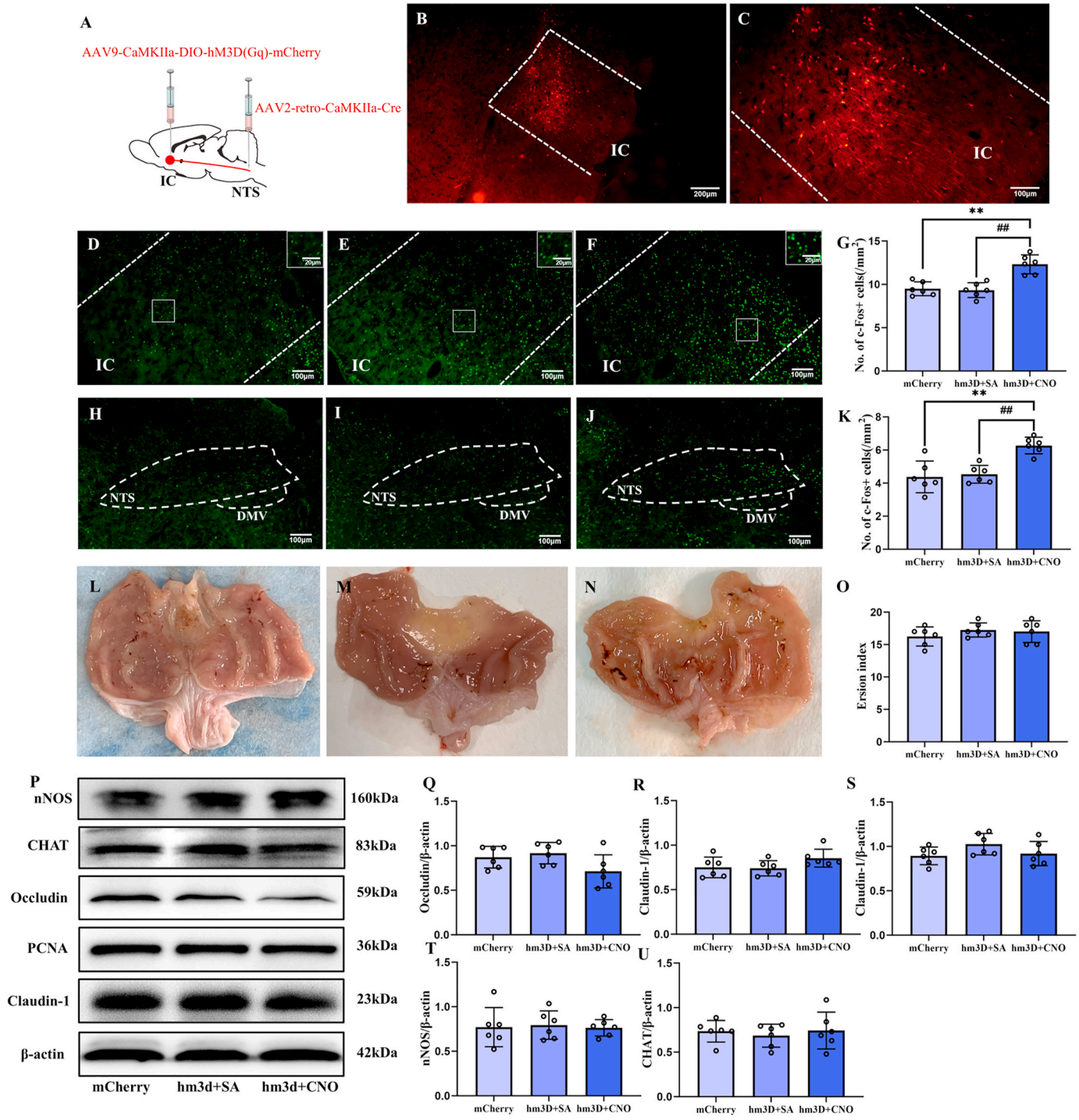

Fig. 7. Effect of activation of the IC-NTS glutamatergic pathway on RWIS-induced gastric mucosal damage. A: Schematic of virus injection; B: viral expression in the IC (40 ×) scale bar, 200 μm; C: viral expression in the IC (100 ×) scale bar,100 μm; D: c-Fos expression in RWIS rats treated with CaMKIIa-mCherry in the IC; E–F: c-Fos expression in RWIS rats in the IC of the CaMKIIa-hm3d + saline- or CNO-injected groups (100 ×). scale bar,100 μm, c-Fos in a rectangle were magnified to a higher magnification (400 ×); scale bar, 20 μm; G: The number of c-Fos-IR neurons in the insul was quantified. compared with mCherry group, *: $P < 0.05$, **: $P < 0.01$, compared with hm3d + SA group, #: $P < 0.05$, ##: $P < 0.01$ (n = 6); H: c-Fos expression in RWIS rats treated with CaMKIIa-mCherry in the NTS; I–J: c-Fos expression in RWIS rats in the NTS of the CaMKIIa-hm3d + saline- or CNO-injected groups (100 ×). scale bar,100 μm; K: The number of c-Fos-IR neurons in the NTS was quantified. compared with mCherry group, *: $P < 0.05$, **: $P < 0.01$, compared with hm3d + SA group, #: $P < 0.05$, ##: $P < 0.01$ (n = 6); L: Gastric mucosal damage in RWIS rats treated with CaMKIIa-mCherry; M–N: Gastric mucosal damage in RWIS rats in the IC of the CaMKIIa-hm3d + saline- or CNO-injected groups; O: Quantification of erosion index (EI). compared with mCherry group, *: $P < 0.05$, **: $P < 0.0$, compared with hm3d + SA group, #: $P < 0.05$, ##: $P < 0.01$ (n = 6); P: Western blot of Occludin, Claudin-1, PCNA, NOS and CHAT protein expression in different groups; Q–U: Quantification of the relative average grayscale value of Occludin/β-actin, Claudin-1/β-actin, PCNA/β-actin, NOS/β-actin and CHAT/β-actin. compared with the mCherry group, *: $P < 0.05$, **: $P < 0.01$, compared with hm3d + SA group, #: $P < 0.05$, ##: $P < 0.01$ (n = 6).

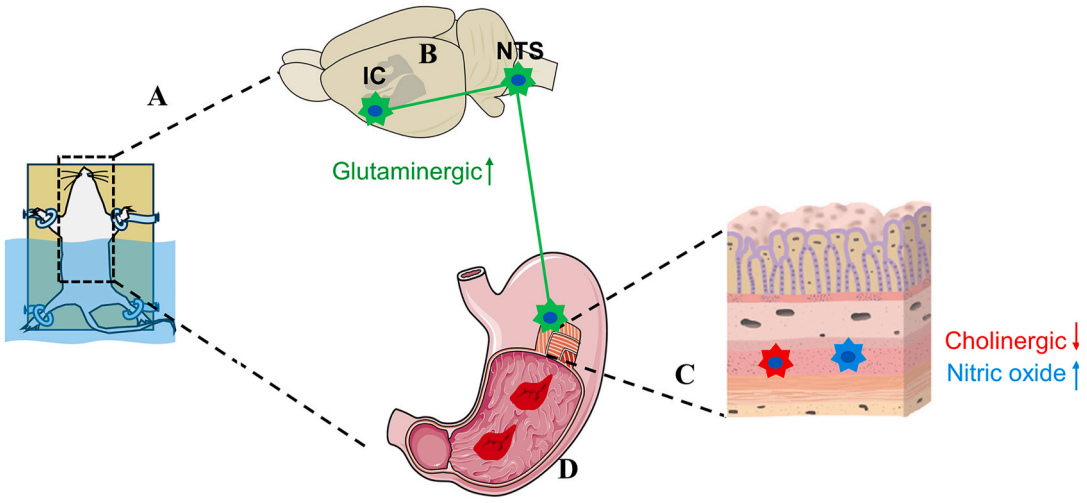

Fig. 8. The IC-NTS glutaminergic pathway involved in RWIS-induced gastric mucosal damage. A: Restraint water-immersion stress triggers activation of IC glutamatergic neurons. B: glutaminergic neurons in IC activated neurons in NTS. C: A reduction in the secretion of the excitatory neurotransmitter acetylcholine and an increase in the secretion of the inhibitory neurotransmitter NO in the gastric intermuscular plexus. D: Impaired gastric function and ultimately resulting in damage to the gastric mucosa.

administration, Methodology, Investigation. **Xinyu Li:** Project administration, Investigation, Data curation. **Yuanyuan Li:** Project administration, Methodology, Data curation. **Xuehan Sun:** Resources, Project administration, Investigation. **Yuxue Wang:** Validation, Methodology, Data curation. **Tong Lu:** Software, Methodology, Investigation. **Dongqin Zhao:** Validation, Resources, Methodology, Investigation. **Xiaoli Ma:** Writing – review & editing, Visualization, Validation, Supervision, Project administration, Conceptualization. **Haiji Sun:** Writing – review & editing, Validation, Supervision, Project administration, Methodology, Investigation, Funding acquisition, Conceptualization.

Funding

This research was funded by the National Natural Science Foundation of China (No.: 32170496) and the Natural Science Foundation of Shandong Province (ZR202102180985).

Declaration of competing interest

The authors declare that they have no known competing financial interests or personal relationships that could have appeared to influence the work reported in this paper.

Data availability

The data that support the findings of this study are available on request from the corresponding author.

References

Clifford, B.S., 2002. The central autonomic nervous system: conscious visceral perception and autonomic pattern generation. Annu. Rev. Neurosci. https://doi.org/10.1146/annurev.neuro.25.032502.111311.

Dongqin, Z., Hua, X., Hongchen, S., 2020. Nervous mechanisms of restraint water-immersion stress-induced gastric mucosal lesion. World J. Gastroenterol. https://doi.org/10.3748/wjg.v26.i20.2533.

Elizabeth, M.B., Melissa, G., Washington, M.T., 2016. The many roles of PCNA in eukaryotic DNA replication. Enzymes. https://doi.org/10.1016/bs.enz.2016.03.003.

Emanuela, M., Sturniolo, G.C., Domenico, P., Frisina, N., Walter, F., 2002. Effect of stress on the paracellular barrier in the rat ileum. Gut. https://doi.org/10.1136/gut.51.4.507.

Erik, M., 2011. Gut feelings: the emerging biology of gut–brain communication. Nat. Rev. Neurosci. https://doi.org/10.1038/nrn3071.

Gao, W., Wang, Z., Wang, H., Li, H., Huang, C., Shen, Y., Ma, X., Sun, H., 2021. Neurons and astrocytes in ventrolateral periaqueductal gray contribute to restraint water immersion stress-induced gastric mucosal damage via the ERK1/2 signaling pathway. Int. J. Neuropsychopharmacol. 24 (8), 666–676. https://doi.org/10.1093/ijnp/pyab028.

Guth, P.H., 1992. Current concepts in gastric microcirculatory pathophysiology. Yale J. Biol. Med. 65 (6), 677–688.

Hongyu, L., 2005. Expression of nitric oxide synthase (NOS) in amygdaloid nuclei of rats under stress of exercise-induced fatigue. J. Chengdu Phys. Educ. Instit. https://doi.org/null.

Hugo, C., Neil, A.H., 2013. Visceral influences on brain and behavior. Neuron. https://doi.org/10.1016/j.neuron.2013.02.008.

Jia, R., Xing, H.J., Zhang, X.P., Zhang, X., Jia, C.S.J.A.R., 2017. Effects of different acupuncture and moxibustion methods on plasma NO, NOS and VIP contents and the expression of colonic VIP protein in functional constipation rats, 42 (1), 50–55.

Jing, L., Zhao-Shen, L.I., Guo-Ming, X.U.J.C.J.o.D., 2003. The Effects of Apoptosis and Proliferation on the Pathogenesis of Rat Stress Ulcer.

Levinthal, D.J., Strick, P.L., 2020. Multiple areas of the cerebral cortex influence the stomach. Proc. Natl. Acad. Sci. U. S. A 117 (23), 13078–13083. https://doi.org/10.1073/pnas.2002737117.

Marcelo, A.-R., Sanggyun, K., Todd, P.C., Pedro, M., Fernando, T., 2020. Interoceptive insular cortex participates in sensory processing of gastrointestinal malaise and associated behaviors. Sci. Rep. https://doi.org/10.1038/s41598-020-78200-w.

Melissa, T.G., Cristiane, B., Ivaldo Jesus Almeida, B.-F., Ricardo, B., Aline, F., Carlos, C. C., Ana Carolina, G., Fernando, M.A.C., Fernando, H.F.A., 2022. NMDA receptors in the insular cortex modulate cardiovascular and autonomic but not neuroendocrine responses to restraint stress in rats. Progress Neuro-Psychopharmacol.; Biol. Psychiatr. https://doi.org/10.1016/j.pnpbp.2022.110598.

Mingming, Z., Anqi, G., Kun, C., Jian, W., Pan, W., Xin-Tong, Q., Jianying, G., Hongwei, F., Da-Yu, Z., Shan-Ming, Y., et al., 2022. Glutamatergic synapses from the insular cortex to the basolateral amygdala encode observational pain. Neuron. https://doi.org/10.1016/j.neuron.2022.03.030.

Oluwole, F.S., 2015. Helicobacter pylori: a pathogenic threat to the gastric mucosal barrier. Afr. J. Med. Med. Sci. https://doi.org/null.

Qiang, L.I., Lei, G., Shaoli, C., Guangli, D.U.J.C.A.o.T.C.M., 2017. Effect of Key Herbs Compatibility in Buzhong Yiqi Decoction on Gastrointestinal Propulsion and Plasma Content of Ghrelin,Nitric Oxide and Vasoactive Intestinal Peptide in Spleen Deficiency Rats.

Richard, J.B., Michael, P.K., Chamberlin, A.R., 1999. A pharmacological review of competitive inhibitors and substrates of high-affinity, sodium-dependent glutamate transport in the central nervous system. Curr. Pharm. Des. https://doi.org/10.2174/1381612805052301101012 59.

Rodrigo, B., Julio, E.C., 1980. A search for differential polypeptide synthesis throughout the cell cycle of HeLa cells. Journal of Cell Biology. https://doi.org/10.1083/jcb.84.3.795.

Rodrigo, B., Stephen, J.F., Jaime, B., Peter Mose, L., Jorge, A., Julio, E.C., 1981. Identification of a nuclear and of a cytoplasmic polypeptide whose relative proportions are sensitive to changes in the rate of cell proliferation. Exp. Cell Res. https://doi.org/10.1016/0014-4827(81)90009-4.

Shun-Wu, X., 2009. Study on NO/NOS content of serum and brain tissue in cerebral ischemia-reperfusion injury rats. China Modern Doctor https://doi.org/null.

Silvia, G., None Jacob, M.H., Andrew, J.T., Joel, C.G., 2020. Central afferents to the nucleus of the solitary tract in rats and mice. J. Comp. Neurol. https://doi.org/10.1002/cne.24927.

Stelios, F.A., Ismini, P., Aristidis, S.C., 2011. Enterocytes' tight junctions: from molecules to diseases. World J. Gastrointest. Pathophysiol. https://doi.org/10.4291/wjgp.v2.i6.123.

Sun, H., Zhao, P., Liu, W., Li, L., Ai, H., Ma, X., 2018. Ventromedial hypothalamic nucleus in regulation of stress-induced gastric mucosal injury in rats. Sci. Rep. 8 (1), 10170. https://doi.org/10.1038/s41598-018-28456-0.

Toshikatsu, O., Akira, U., Kiyoshi, O., Masayoshi, N., 1990. Site-specific formation of gastric ulcers by the electric stimulation of the left or right gastric branch of the vagus nerve in the rat. Scand. J. Gastroenterol. https://doi.org/10.3109/00365529008999223.

Udo, H., Schuetz, A., 2019. Structural features of tight-junction proteins. Int. J. Mol. Sci. https://doi.org/10.3390/ijms20236020.

Yanwei, L., Wei, L., Songtao, W., Yinan, G., Baomin, D., Zhongxi, L., Luis, U., Shenjun, W., Zhifang, X., Yi, G., 2022. The autonomic nervous system: a potential link to the efficacy of acupuncture. Front. Neurosci. https://doi.org/10.3389/fnins.2022.1038945.

Ying, C., Xiaoyuan, L., Guangxian, C.J.C.A.o.T.C.M., 2014. Effects of Simo Decoction on Ghrelin Nos in Cold-Constraint Stressed Mice.

Yu, W., Changwan, C., Ming, C., Kai, Q., Xiaoshu, L., Haiting, W., Jiang, L.-f., Yu, L., Min, Z., Shuang, Q., 2020. The anterior insular cortex unilaterally controls feeding in response to aversive visceral stimuli in mice. Nat. Commun. https://doi.org/10.1038/s41467-020-14281-5.

Yuwei, H., Yuanyuan, Z., Xiuying, L., Han, L., Junping, K.J.J.o.C.P.U., 2017. Advances of Regulatory Effects of Traditional Chinese Medicine on NOS/NO System.

Yuyu, Z., 2009. Comparative study of c-fos expression in rat dorsal vagal complex and nucleus ambiguus induced by different durations of restraint water-immersion stress. Chin. J. Physiol. https://doi.org/10.4077/cjp.2009.amh045.

Yvette, T., Robert, L.S., Takahiro, I., 1989. Central nervous system action of TRH to influence gastrointestinal function and ulceration. Ann. N. Y. Acad. Sci. https://doi.org/10.1111/j.1749-6632.1989.tb46649.x.

Zhang, F.C., Wei, Y.X., Weng, R.X., Xu, Q.Y., Li, R., Yu, Y., Xu, G.Y., 2023. Paraventricular thalamus-insular cortex circuit mediates colorectal visceral pain induced by neonatal colonic inflammation in mice. CNS Neurosci. Ther. null. https://doi.org/10.1111/cns.14534.

Zhou, X.-j., 2004. Investigation of the Changes of Gastrointestinal Hormone and Nitric Oxide Synthetase of Sigmoid Mucosa in Patients with Functional Constipation. Modern Digestion & Intervention https://doi.org/null.

Zimmermann, M., 1986. Ethical considerations in relation to pain in animal experimentation. Acta Physiol. Scand. 128 (Suppl. 554), 221–233.